Mon. Not. R. Astron. Soc. **349,** 641–648 (2004) doi:10.1111/j.1365-2966.2004.07531.x

The old open cluster Trumpler 5: a reddened, metal-poor anticentre cluster

Andrés E. Piatti,[1⋆] Juan J. Clariá[2] and Andrea V. Ahumada[2]
[1]*Instituto de Astronomía y Física del Espacio, CC 67, Suc. 28, 1428, Buenos Aires, Argentina*
[2]*Observatorio Astronómico, Laprida 854, 5000 Córdoba, Argentina*

Accepted 2003 December 8. Received 2003 November 27; in original form 2003 August 13

ABSTRACT

CCD observations in the Johnson V, Kron–Cousins I and the Washington system C and T_1 passbands have been used to generate colour–magnitude diagrams (CMDs) reaching down to $V \sim 21.0$ mag and $T_1 \sim 19.0$ for Trumpler 5, an old open cluster located towards the Galactic anticentre. Our data analysis confirms the existence of non-uniform extinction over the face of the cluster, the mean $E(V-I)$ and $E(C-T_1)$ values being 0.80 ± 0.05 and 1.17 ± 0.15, respectively. Through comparison of the cluster CMDs with theoretical isochrones of the Geneva group, Washington Standard Giant Branches and measures of δV and δT_1 indices, we derive the following values for the cluster apparent distance modulus, age, and metallicity: $V - M_V = 13.80 \pm 0.30$ (corresponding to a distance from the Sun of 2.4 ± 0.5 kpc and 0.04 kpc above the Galactic plane), $t = 5.0 \pm 0.5$ Gyr and [Fe/H] $= -0.30 \pm 0.15$. We estimate the cluster angular radius to be about 7.7 arcmin (= 5.4 pc) from star counts carried out within and outside the cluster field.

Key words: techniques: photometric – open clusters and associations: general – open clusters and associations: individual: Trumpler 5.

1 INTRODUCTION

This work belongs to a series of papers devoted to some unstudied or poorly studied open clusters, located in different Galactic radii, for which we measure in a homogeneous way the distance, age, reddening and metallicity, using good-quality CCD photometry in the Johnson V, Kron–Cousins I and C, T_1 Washington systems. We have already reported results on the relatively young and metal-poor open cluster NGC 2194 (Piatti, Clariá & Ahumada 2003a, hereafter Paper I) and the intermediate-age open cluster NGC 2627 (Piatti, Clariá & Ahumada 2003b).

As is well known, intermediate-age and old open clusters cover a large range of distances, metallicities and ages (Friel 1995; Friel et al. 2002). This characteristic justifies their use in investigations of the chemical and dynamical evolution of our Galaxy. Open clusters provide unique information on the chemical abundances and gradients in the disc (e.g. Friel & Janes 1993; Piatti, Clariá & Abadi 1995; Chen, Hou & Wang 2003), on the average stellar ages and radial velocities at different Galactic radii (e.g. Janes & Phelps 1994) and on the interactions between thin and thick discs (e.g. Spitzer 1988). Investigations focusing on the age–metallicity relation for the Galaxy (e.g. Strobel 1991) require high-quality data on the greatest possible number of intermediate-age and old open clusters. Nevertheless, unluckily, many open clusters are destroyed as a consequence of interactions with molecular clouds on time scales of a few hundred million years or less (Spitzer 1988). Thus, few very old clusters are believed to have survived up to the present stage.

The faint, rich open cluster Trumpler 5 (Tr 5), IAU designation C0634+094, was discovered and catalogued by Trumpler (1930). This cluster, also known as Cr 105 (Collinder 1931), is located towards the Galactic anticentre in a rich star field in Monoceros at equatorial coordinates $\alpha = 6^{\rm h}34^{\rm m}$, $\delta = +9^\circ 29'$(2000.0) and Galactic coordinates $l = 202\overset{\circ}{.}9$ and $b = +1\overset{\circ}{.}1$. Ruprecht (1966) described it as belonging to Trumpler (1930) class II3r, i.e. a rich, detached open cluster with a medium range in the brightness of the stars. This object, lying in the sky projected against distant opaque clouds of interstellar gas, was included by King (1964) in a list of clusters that appeared to be old on the basis of their appearance on the Palomar Observatory Sky Survey (POSS) prints. Tr 5 is particularly interesting as it contains a very red ($B - V \approx 6.1$) object, V593 Mon, identified by Kalinowski (1974) and Kalinowski, Burkhead & Honeycutt (1975) as a possible carbon-star member of the cluster. Piccirillo, Kalinowski & Wing (1977) also identified three M giants, three K giants and another relatively hot carbon star. Both a photographic study by Dow & Hawarden (1970) and a photographic and photoelectric one by Kalinowski (1979) revealed that this is indeed an old, highly reddened open cluster. However, while Dow & Hawarden (1970) derived a reddening $E(B-V) = 0.80$ and a distance $d = 2.4$ kpc, Kalinowski (1979) obtained 0.64 and 1.0 kpc, respectively. Kalinowski's data also show that Tr 5 is

⋆E-mail: andres@iafe.uba.ar (AEP); claria@mail.oac.uncor.edu (JJC); andrea@mail.oac.uncor.edu (AVA)

differentially reddened, the mean visual absorption across the cluster field being approximately 2.1 magnitudes. Janes & Adler (1982) used Kalinowski's data, thereby producing respective estimates of $E(B-V)=0.80$ and $V-M_V=14.40$ for the reddening and apparent distance modulus of the cluster, respectively. Phelps, Janes & Montgomery (1994) defined the morphological age index δV as the magnitude difference between the main-sequence turnoff and the clump in the $(V, V-I)$ colour–magnitude diagram, deriving $\delta V = 2.2$ for Tr 5 from Kalinowski (1979) data. This value implies an age of 5.6 Gyr (Janes & Phelps 1994), thus making the cluster very old. Although Tr 5 has a relatively small angular diameter of about 12 arcmin (Kalinowski 1975), which makes it a good target for CCD camera analysis, the only CCD photometric study up to date was performed by Kaluzny (1998), who obtained *BVI* photometry within a field of about 11.6×11.6 arcmin. His cluster colour–magnitude diagram (CMD) displays a well-populated giant branch and a clump of stars near $V=15.0$ and $B-V=1.5$. By assuming solar metal content, he derived a colour excess $E(B-V)=0.58$, a distance $d=3.0$ kpc and an age of 4.1 Gyr, slightly lower than that of M67 (Carraro & Chiosi 1994). He was also able to estimate the lower limit for the cluster total mass as 3000 solar masses. The angular diameter estimated by Kaluzny (1998) from star counts in different annuli around the cluster centre is about $12'$. More recently, Kim & Sung (2003) presented a new analysis of the *BVI* data obtained by Kaluzny (1998). They derived $E(B-V)=0.60\pm0.10$ from the mean $(B-V)$ colour of the red giant clump. Using theoretical isochrones computed by Bertelli et al. (1994), they have also estimated a distance $d=3.4\pm0.3$ kpc, a metallicity $[\mathrm{Fe/H}]=-0.30\pm0.10$, and an age of 2.4 ± 0.2 Gyr.

We report here the results obtained from high-quality CCD VI_{KC} photometry up to $V\approx21.0$ and CCD photometry in the C and T_1 bands of the Washington system up to $T_1\approx19.0$ in the cluster field. These data are employed to make a new independent determination of reddening, distance, age and metallicity of Tr 5.

In Section 2 we briefly describe the observations and the data reduction. In Section 3 we present a description and analysis of the main features appearing in the different photometric diagrams, while in Section 4 and through the fitting of theoretical isochrones, we determine the cluster reddening, distance, age and metallicity. A discussion of the present findings for Tr 5 is given in Section 5. Finally, a brief summary of our main conclusions is presented in Section 6.

2 OBSERVATIONS AND REDUCTIONS

The observations were carried out with the Cerro Tololo Inter-American Observatory (CTIO) 0.9-m telescope in 1997 December, with the 2048×2048 pix CCD Tektronix 2K #3, as described in Paper I for the open cluster NGC 2194. The scale on the chip is 0.40 arcsec pixel^{-1}, yielding an area of 13.6×13.6 arcmin^2. The filters used were the Johnson V, Kron–Cousins I and Washington system (Canterna 1976) C and T_1. The CCD was controlled by the CTIO ARCON 3.3 data acquisition system in the standard quad amplifier mode operating at a gain of 5 e$^-$ ADU^{-1} with a readout noise of 4e$^-$. We obtained one 15-s and two 45-s V exposures, two 15-s and one 50-s I exposures, two 300-s C exposures and two 10-s T_1 exposures for Tr 5. The seeing was typically 1.5 arcsec during the observing night.

Fig. 1 shows a schematic finding chart of the observed cluster field built with all measured stars in the V-band. In this paper, as in Paper I, we calibrated the observations in the VI_{KC} and Washington systems through the observation of numerous standard stars from the lists of Landolt (1992) and Geisler (1996) covering a wide range in colour. The data were reduced at the Observatorio Astronómico de la Universidad Nacional de Córdoba (Argentina) with stand-alone version of DAOPHOT II (Stetson 1987), after trimming, bias subtracting, and flat-fielding the images at CTIO. Details on the reduction and calibration procedures are provided in Paper I.

Table 1 gives in succession a running star number of the observed stars, X and Y coordinates in pixels (Fig. 1), V magnitudes and $V-I$ colours, along with the corresponding observational errors $\sigma(V)$ and $\sigma(V-I)$, the number of observations, and the star identification given by Kaluzny (1998). The construction of this table is explained in Paper I. A partial section of this table is offered here for guidance in terms of its form and content. Full display of this table will be available upon request to the first author of this paper. Following the same procedure, we built Table 2 – also available upon request to the first author – including not only the T_1 magnitudes and $C-T_1$ colours for all the measured stars, but also the X and Y coordinates and the corresponding photometric errors.

Fig. 2 shows the trend of the V magnitude and $V-I$ colour errors with V provided by DAOPHOT for Tr 5. Fig. 3 illustrates how our V magnitudes and $V-I$ colours differ from those obtained by Kaluzny (1998) as a function of V. Offsets of $\Delta(V_{\mathrm{our}}-V_{\mathrm{K98}})=0.010\pm0.054$ and $\Delta[(V-I)_{\mathrm{our}}-(V-I)_{\mathrm{K98}}]=0.004\pm0.064$ have been computed from 594 stars measured in common.

3 *VI* AND *CT*$_1$ COLOUR–MAGNITUDE DIAGRAMS ANALYSIS

The result of the finally calibrated *VI* photometry is shown in the CMD of Fig. 4, which includes all the stars measured in the field of Tr 5. The most prominent feature is a broad main sequence (MS) extending roughly from $V=16.3$ down to 21 mag. The width of the MS generally reaches 0.4 mag, suggesting the existence of differential reddening across the cluster field. This can also be inferred from the orientation of the red giant clump (RGC) located at $(V, V-I)\sim(15.0, 1.8)$ mag, the clear tilted placement of which follows the direction of the reddening vector. On the other hand, contamination from field stars cannot be ruled out either. Several stars located above the turn-off and bluer than $V-I\approx1.3$ appear to be good candidates for blue stragglers. One of the most evident signatures is the bright upper field MS which appears to join the lower envelope of the cluster MS. A clump of field giants is also visible at $V\sim14$ mag.

To disentangle the cluster fiducial characteristics of the CMD, we evaluated the influence of photometric errors, field contamination and differential reddening across the cluster field. Photometric errors are correlated with the number of measures per star. 56 per cent of the total number of measured stars have three measures of their V magnitudes and $V-I$ colours and expand approximately from the brightest limit down to $V=20$, while 17 and 27 per cent of the measured stars have two and one measures and cover V ranges from 18 to 20.5 mag and from 19.5 until the photometric limit, respectively. According to this census, the MS is mainly defined by stars with three measures, the errors of which are those shown in Fig. 2, i.e. $\sigma_V\leqslant0.05$ mag for $V=20$ and ≈0.01 mag for $12<V<17$, and $\sigma_{V-I}\leqslant0.05$ mag for $V=19$ and 0.01 mag for $V\leqslant16$. Thus, the scatter produced by photometric errors is negligible in comparison with the colour width of the MS.

To evaluate the level of field star contamination in the CMD, we first determined the cluster centre and its extension, and then built different CMDs with stars distributed in the cluster and field regions.

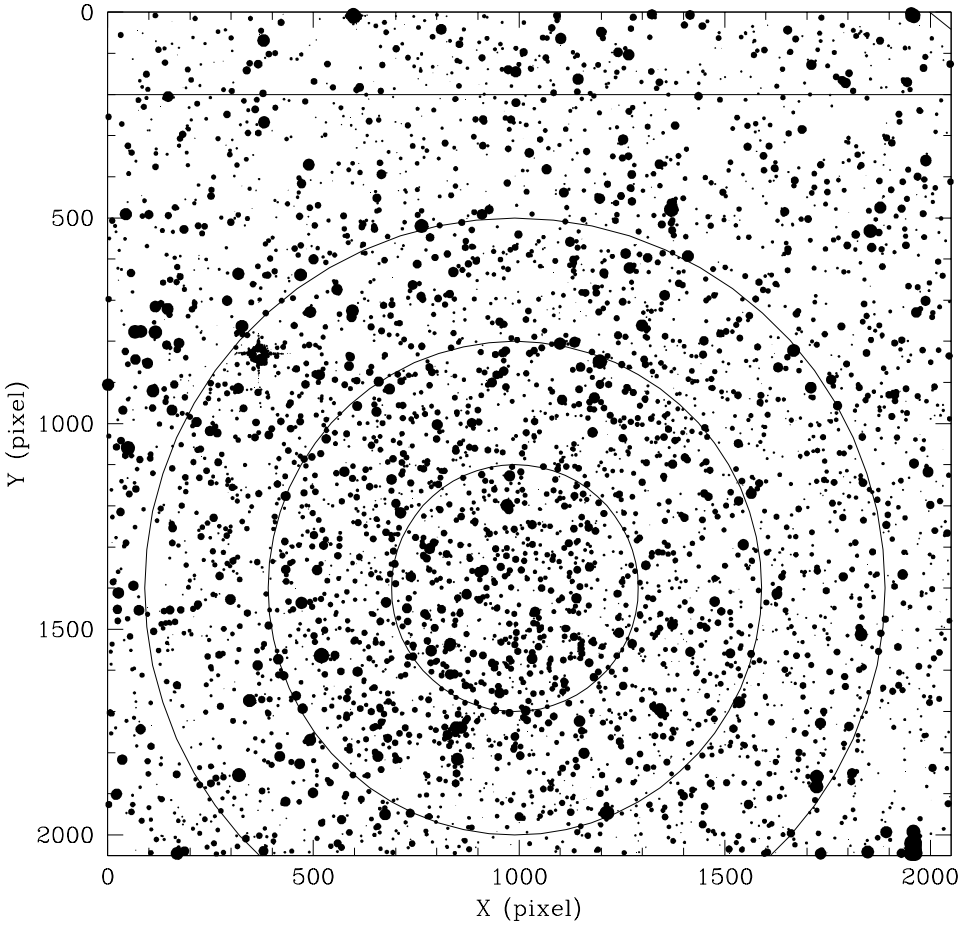

Figure 1. Schematic finding chart of the stars observed in the field of Tr 5. North is up and east is to the left. The sizes of the plotting symbols are proportional to the V brightness of the stars. Three concentric circles around the cluster centre and an horizontal line delimiting the southern limit of the star field area are also drawn.

Table 1. CCD *VI* data of stars in the field of Tr 5.

Star	X (pixel)	Y (pixel)	V (mag)	$\sigma(V)$ (mag)	$V-I$ (mag)	$\sigma(V-I)$ (mag)	n	ID (K98)
1	1953.723	2.813	13.588	0.226	1.846	0.257	1	
2	1323.065	4.915	15.154	0.001	0.828	0.004	2	
3	426.582	5.142	21.063	0.092	2.541	0.120	1	
4	1088.718	5.195	19.086	0.109	1.357	0.032	3	
5	1414.934	5.263	19.757	0.198	2.502	0.242	1	
.	.	.	.	.	.	.	.	
.	.	.	.	.	.	.	.	
.	.	.	.	.	.	.	.	

Note: (X, Y) coordinates correspond to the reference system of Fig. 1. Magnitude and colour errors are the standard deviations of the mean, or the observed photometric errors for stars with one measurement.

Projected stellar density profiles were constructed along the X and Y axes to derive the cluster centre using intervals of different sizes. The different bin sizes were used to monitor the evolution of the star count noise, originated by stellar density fluctuations particularly noticeable in star fields affected by differential extinction. For each pair of X and Y projected stellar density profiles, we fitted Gaussian functions to obtain the value of the cluster centre. During the fits we took care of spurious peaks caused by small concentrations of stars

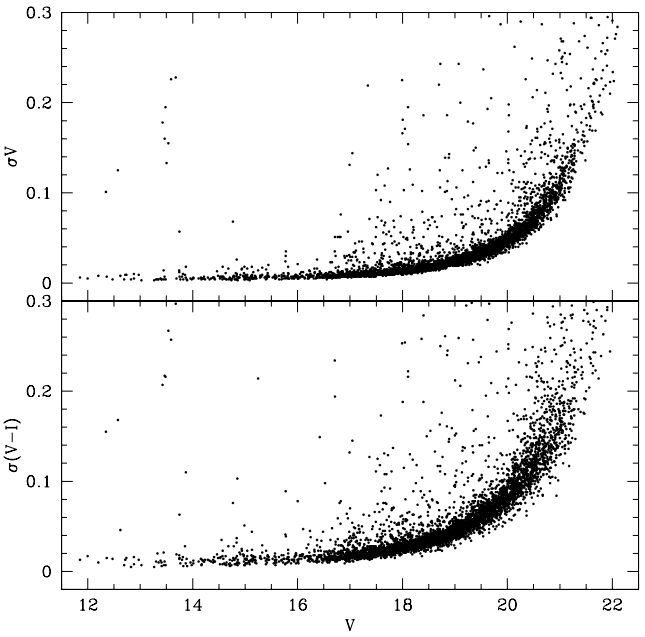

Figure 2. Magnitude and colour photometric errors as a function of V.

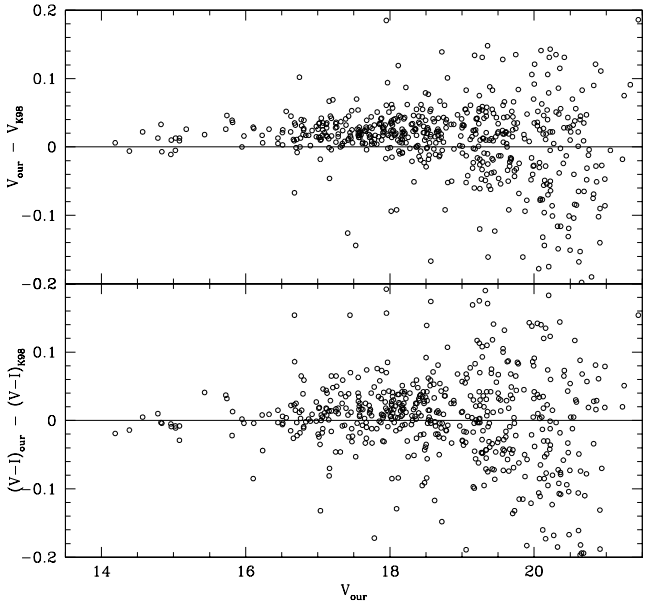

Figure 3. Differences between our V magnitudes and $V - I$ colours and those obtained by Kaluzny (1998) as a function of V.

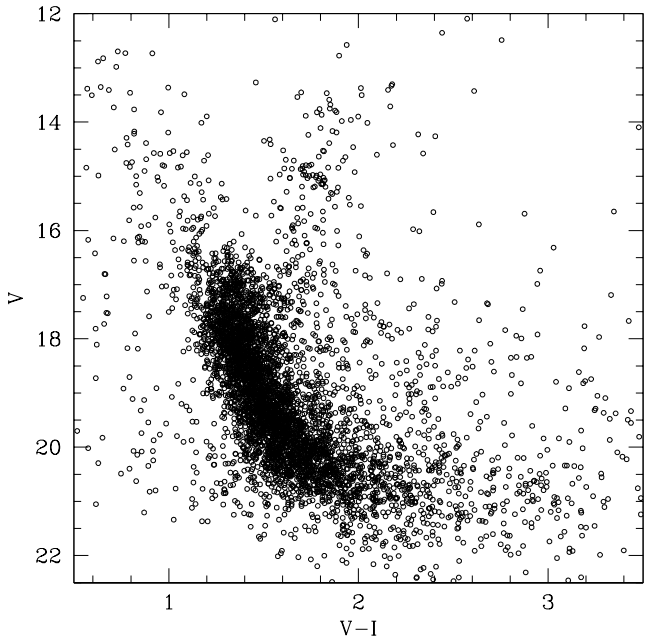

Figure 4. (V,$V - I$) colour–magnitude diagram for stars observed in the field of Tr 5.

spread through the field. Finally, we averaged five different centres derived from density profiles built with bins of 30 up to 70 pixels wide. The adopted position of the cluster centre is $(X_C, Y_C) = (990 \pm 25, 1400 \pm 25)$ pixels.

With the aim of estimating the cluster angular radius, we performed star counts in boxes of 30 pixels per side, instead of counting stars lying in concentric rings around the cluster centre. This procedure facilitated adequate sampling of the star distribution normalized to the unit area as far as the boundary of the observed field. Thus, the star density for a given radius r was obtained by adding up stars counted in those boxes that lie within a ring Δr centred at r. In

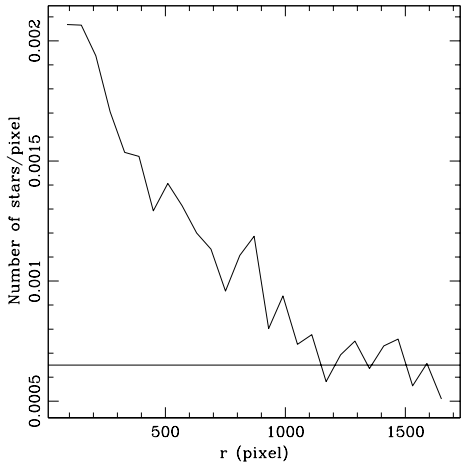

Figure 5. Stellar density profile centred at $(X_C, Y_C) = (990, 1400)$ pixels for stars observed in the field of Tr 5.

Fig. 5 we present the radial profile obtained using $\Delta r = 60$ pixels. No difference was found when making the figure using a different Δr value between 30 and 70 pixels. According to Fig. 5, most of the cluster stars appear to be confined within a radius of $r_C = 1150 \pm 50$ pixels, equivalent to 7.7 ± 0.3 arcmin, which was adopted as the cluster angular radius. Upon this assumption, we used as field star area a fringe of 200 pixels wide along the X axis at the top of the observed field. Fig. 1 shows the contours of this area.

Fig. 6 shows four CMDs extracted from three circular regions centred on the cluster and from the surrounding field, respectively. The extracted regions are labelled at the top of each panel. We also drew the reddening vector for an $E(B - V)$ colour excess of 0.5 mag. When comparing the CMDs of the cluster central region (upper left-hand panel) and that of the field (lower right-hand panel), some differences come up: (i) the RGC of the $r < 300$ pix CMD is $\sim$1.5 mag fainter than that associated to the field; (ii) the cluster

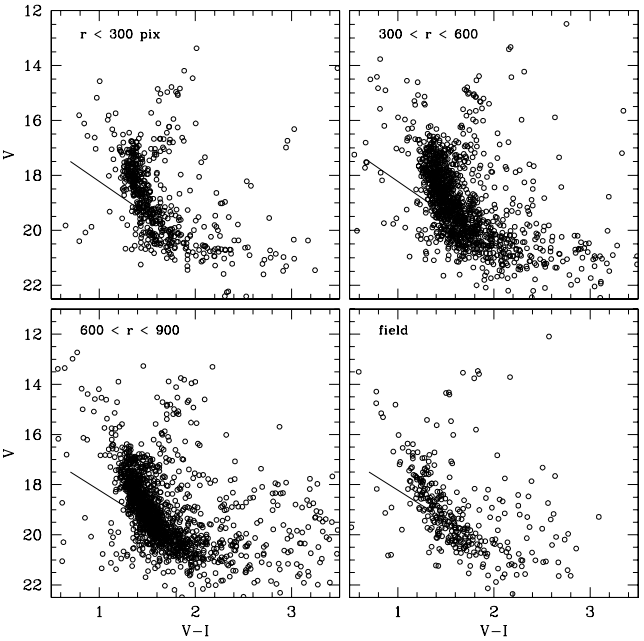

Figure 6. (V, $V - I$) colour–magnitude diagram for stars observed in different extracted regions as indicated in each panel. See Section 3 for details.

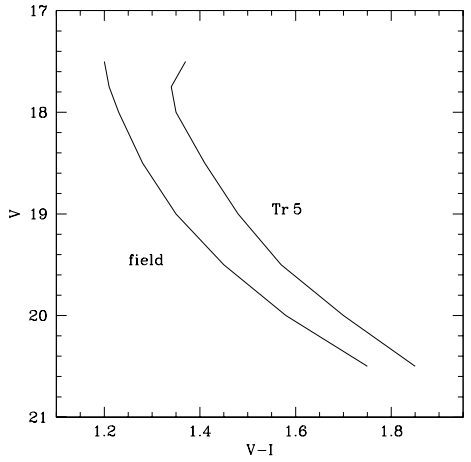

Figure 7. $(V, V-I)$ colour–magnitude diagram with the fiducial main sequences of both Tr 5 and its surrounding field.

CMD does have a more evolved upper MS, its lower envelope also being in general different. We plotted both MSs in Fig. 7 for comparison purposes. Each curve was traced by joining the midway points of the observed MSs for intervals of 0.5 mag in V. (iii) The field CMD does not present a subgiant branch (SGB), which is clearly visible in the cluster CMD. On the other hand, the intermediate ($300 < r < 600$) and bigger ($600 < r < 900$) circular-extracted CMDs also present MSs with a similar curvature to that of the innermost cluster region as well as RGCs and stars developing the SGB. However, two remarkable features differentiate the intermediate and bigger circular-extracted CMDs from the $r < 300$ pix CMD. Firstly, the RGC for the outermost cluster regions is tilted, oriented parallel to the direction of the reddening vector. Secondly, the MS appears to broaden as the distance from the cluster centre increases, doubling its colour width for $r > 600$ pixels. Scatter in the direction of the reddening vector is also visible for SGB stars.

Based on the fact that field stars appear to be spread out not only in the assigned field area ($0 < Y < 200$ pixels) but also through the whole field, we statistically removed such contamination aiming at studying the magnitude and spatial distribution pattern of the differential reddening across the cluster field. For this purpose, we counted the number of stars in boxes of $[\Delta(V-I), \Delta V] = (0.1, 0.5)$ mag in the field CMD of Fig. 6 (lower right-hand panel), and subtracted per unit area the same number of stars per colour–magnitude bin in the entire field. Hence, we obtained a CMD with all the measured cluster stars virtually free from the contamination of field stars. Given that this is a statistical procedure, some field interlopers should be expected in the resulting cluster CMD. Likewise, a scarce number of cluster stars should also lie in the field star area, although neither of these two situations significantly affects the features of the cluster CMD. For the sake of illustration, in Fig. 8 we present the field-star cleaned circular-extracted CMDs. The lower right-hand panel shows that weak evidence of the cluster MS appears to arise at $r = 1100$–1200 pixel. The remaining circular-extracted CMDs keep the cluster features described above, which in turn present now a better defined lower MS envelope. Note also that the differences between the inner and outermost extracted cluster CMDs are still visible, namely the change in the orientation of the RGC and the colour expansion of the MS.

Fig. 9 reproduces Fig. 1 for MS cluster stars distributed in different $\Delta(V-I)$ colour ranges measured from the fiducial cluster MS (Fig. 7). The plotted stars are those not subtracted by the field-star cleaning process. The circles have the same radii as in Fig. 1. Panels from left to right and from top to bottom in Fig. 9 correspond to $\Delta(V-I) = -0.05$–0.05 mag; 0.05–0.15 mag; 0.15–0.30 mag, and >0.30 mag, respectively. The upper left-hand panel reveals that stars with relatively small photometric errors and/or the lowest colour excesses are mostly distributed in the cluster core

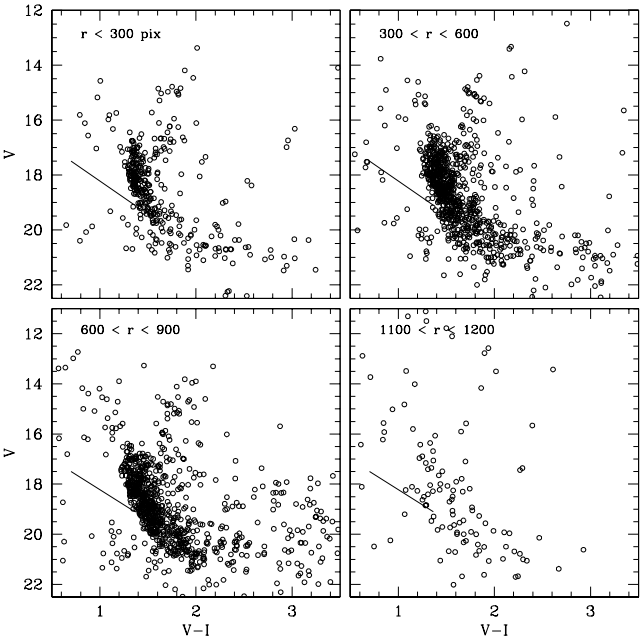

Figure 8. Field-star cleaned $(V, V-I)$ colour–magnitude diagram for stars observed in different extracted regions as indicated in each panel. See Section 3 for details.

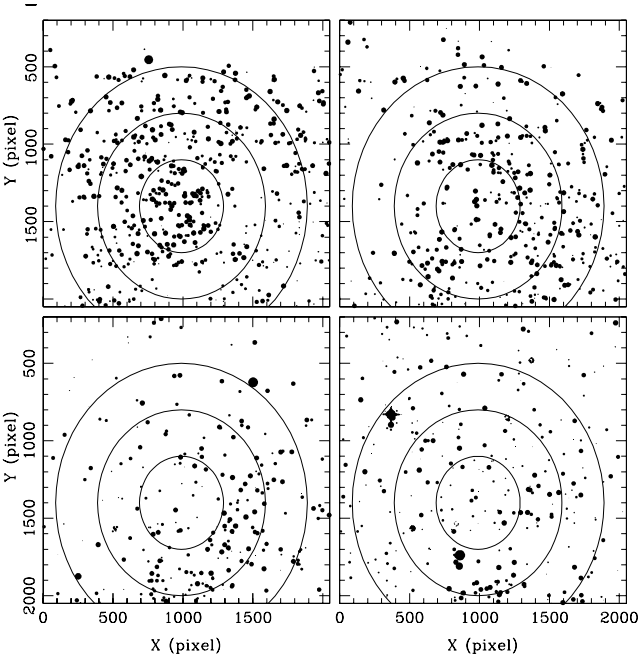

Figure 9. Schematic finding charts of the stars distributed inside the $\Delta(V-I) = \pm 0.05$ mag shifted MS (upper left-hand panel), between 0.05 mag and Burki's limit MSs (right-hand panel), from Burki's limit until $\Delta(V-I) = 0.30$ shifted MS (lower left-hand panel), and beyond $\Delta(V-I) = 0.30$ shifted MS (lower right-hand panel). North is up and east is to the left.

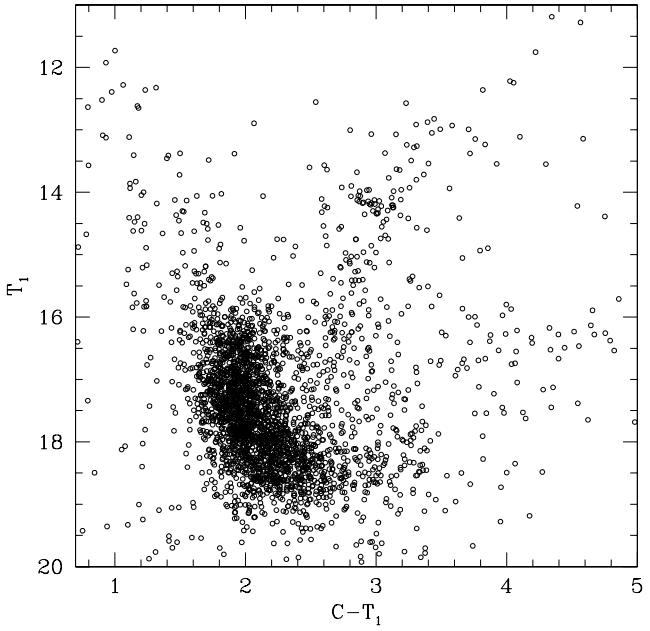

Figure 10. $(T_1, C - T_1)$ colour–magnitude diagram for stars observed in the field of Tr 5.

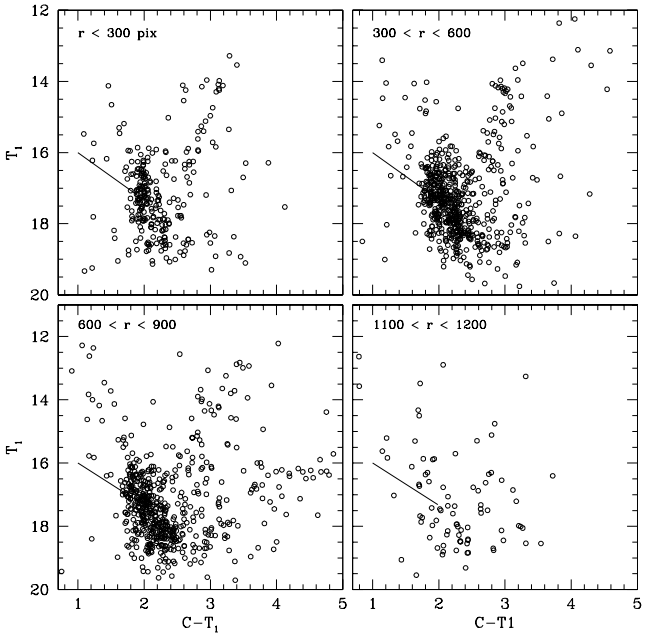

Figure 11. Field star cleaned $(T_1, C - T_1)$ colour–magnitude diagram for stars observed in different extracted regions as indicated in each panel. See Section 3 for details.

region ($r < 300$ pixel) as well as in the northeastern half of the observed field. Stars distributed within $\Delta(V - I) = 0.05$–0.15 mag (upper right-hand panel) are surprisingly located in regions with a relative absence of less reddened stars. Notice that by shifting redwards the fiducial cluster MS in $\Delta(B - V) = 0.11$, the lower limit estimated by Burki (1975) for clusters with differential reddening is reached, which corresponds to $\Delta(V - I) = 0.15$, if a value of 1.33 for the $E(V - I)/E(B - V)$ ratio (Cousins 1978) is adopted. Stars with reddenings between once and twice that of the Burki's value and those with larger $E(V - I)$ colour excesses are depicted in both lower left-hand and right-hand panels, respectively. They show that an obscure cloud of interstellar matter as large as a quarter of ring of ∼300 pixels wide at 450 pixels from the cluster centre interposes in the line of sight towards the southwestern side of the cluster, and that the highest reddened group of stars is found towards the south.

The resulting CMD with all the measured stars in the CT_1 Washington system is shown in Fig. 10. We obtained T_1 magnitudes and $C - T_1$ colours for approximately 40 per cent fewer stars than in the *VI* photometry, because of the relatively brighter limiting magnitude reached with the Washington C passband. For this reason, we based the choice of the parameters involved in the CMD analysis (e.g. cluster centre, circular extractions, field area) on the *VI* photometry instead of on the CT_1 one. However, even though a smaller number of stars were measured in the Washington system, the broad MS, the SGB stars and the tilted RGC are also clearly identified in Fig. 10. We thus accounted for field contamination following the same precepts applied to the *VI* data, and plotted the final cleaned circular-extracted CMDs in Fig. 11. The radii for the distinct-extracted CMDs are labelled at the top of each panel, which also show the reddening vector corresponding to an $E(B - V)$ colour excess of 0.5 mag. As can be seen, the same conclusions about the cluster features inferred from the *VI* data can also be drawn from Fig. 11. We note, in addition, that the red giant branch looks better defined in the $r < 300$ pixels $(T_1, C - T_1)$ CMD than in the respective $(V, V - I)$ CMD.

4 CLUSTER FUNDAMENTAL PARAMETERS

To estimate the reddening, distance, age and metallicity of Tr 5, we decided to use the cleaned innermost extracted CMDs, since they are practically unaffected from differential interstellar extinction. We also based our fundamental cluster parameters determination on the availability of theoretical isochrones recently computed for both *VI* and CT_1 photometric systems. Particularly, we used those isochrones calculated with core overshooting effect by Lejeune & Schaerer (2001). As a first independent-age estimate, which also served as an approach in the selection of a sample of isochrones distributed within an age range around the cluster age, we measured the δV index – the difference in magnitudes between the RGC and the MS turnoff (Phelps et al. 1994) – which in turn converts into an age estimate through the morphological age index (MAI) calibrated by Janes & Phelps (1994). We measured $\delta V = 2.05 \pm 0.15$, which implies a cluster age (MAI) of $4.6^{+1.0}_{-0.7}$ Gyr. On the other hand, since Kaluzny (1998, hereafter K98) and Kim & Sung (2003, hereafter KS03) assumed solar ($Z = 0.02$) and subsolar ($Z = 0.008$) metallicities for Tr 5, we initially decided to use both chemical compositions for the isochrone sets. We then selected isochrones around the derived MAI value for these two different metal abundance levels (Z). The isochrones were individually adjusted to the cluster $(V, V - I)$ CMD until reaching the best match of the turnoff (TO), the MS curvature and red evolved phases. The isochrone that best reproduces the cluster features corresponds to $\log t = 9.70$ ($t = 5.0$ Gyr) and $Z = 0.008$ ([Fe/H] $= -0.40$). For these values we derived an $E(V - I)$ colour excess and a $V - M_V$ apparent distance modulus of 0.80 and 13.80, respectively (note that for $Z = 0.02$ we obtained the same distance modulus and a $E(V - I)$ reddening value 0.10 mag smaller). Their respective uncertainties were estimated from the individual values obtained from the cluster features dispersion. Thus, we estimated $\sigma(t) = 0.8$ Gyr, $\sigma(E(V - I)) = 0.05$ mag, and $\sigma(V - M_V) = 0.30$ mag. By employing the most frequently used values of 1.33 and 3.2 for the $E(V - I)/E(B - V)$ and $A_V/E(B - V)$ ratios, respectively, we obtained an $E(B - V)$ reddening value of

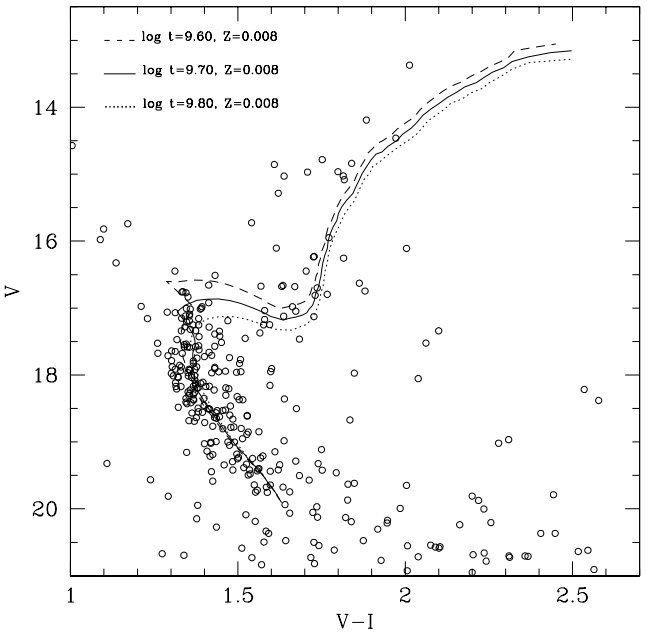

Figure 12. (V,$V-I$) CMD for stars in Tr 5. Isochrones from Lejeune & Schaerer (2001), computed taking into account overshooting, are overplotted.

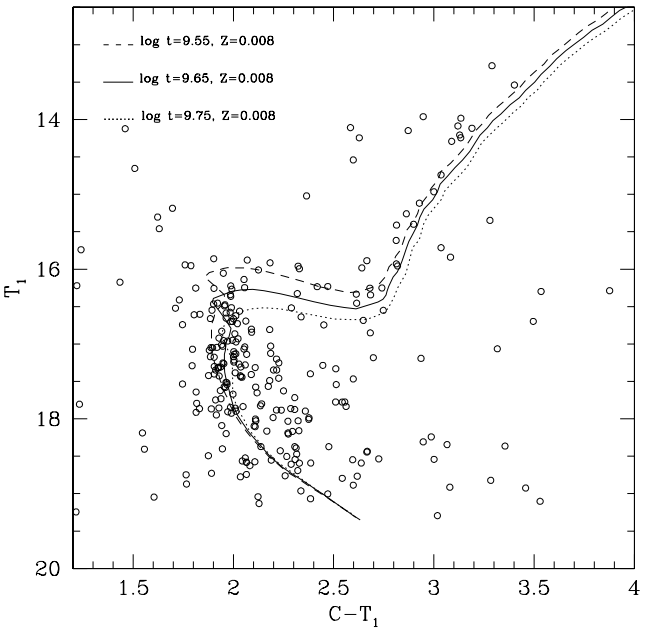

Figure 13. (T_1, $C-T_1$) CMDs for stars in Tr 5. Isochrones from Lejeune & Schaerer (2001), computed taking into account overshooting, are overplotted.

0.60 ± 0.04 mag and a distance from the Sun of 2.4 ± 0.5 kpc. Fig. 12 shows three different isochrones shifted by $\Delta(V-I)=0.80$ and $\Delta V=13.80$, which illustrate the fitting procedure.

We used the same scheme of analysis as described above for estimating the cluster properties from the cleaned $r<300$ pixels extracted (T_1, $C-T_1$) CMD, using in this case the δT_1 index as age reference (Geisler et al. 1997). We measured $\delta T_1=2.40\pm0.14$, which implies a cluster age of $4.3^{+0.6}_{-0.4}$ Gyr. The best fit is now achieved when matching the isochrone of $\log t=9.65$ ($t=4.4$ Gyr) and $Z=0.008$ with $E(C-T_1)=1.17$ and $T_1-M_{T_1}=13.65$. The estimated errors for the cluster parameters are: $\sigma(t)=0.8$ Gyr, $\sigma(E(C-T_1))=0.15$, and $\sigma(T_1-M_{T_1})=0.25$ mag. Similarly, by using $E(C-T_1)/E(B-V)=1.97$ and $A_{T_1}/E(B-V)=2.62$ (Geisler, Lee & Kim 1996), we derive $E(B-V)=0.60\pm0.08$ mag and $d=2.6\pm0.7$ kpc for the cluster. Fig. 13 shows the isochrone for the adopted cluster age and metallicity (solid line) and two additional isochrones for comparison purposes. The fundamental parameters estimated from both photometries resulted in excellent agreement, because of which we adopted those coming from the *VI* data for the subsequent analysis.

We finally made an independent determination of the cluster metallicity using the [M_{T_1},($C-T_1$)] plane with the standard giant branches (SGBs) of Geisler & Sarajedini (1999). They demonstrated that the metallicity sensitivity of the SGBs (each giant branch corresponds to an iso-abundance curve) is three times higher than that of the V, I technique (Da Costa & Armandroff 1990) and that, consequently, it is possible to determine metallicities three times more precisely for a given photometric error. Fig. 14 shows the cluster giants for the cleaned innermost extracted CMD with the SGBs superimposed. From this figure we derived an observed cluster metallicity of [Fe/H] $=-0.50\pm0.10$ dex. However, in view of the well known age–metallicity degeneracy, we followed the prescriptions described by Geisler et al. (2003) and applied a correction of +0.20 dex to the observed metallicity. Thus, we finally obtained [Fe/H] $=-0.30\pm0.15$ for the cluster metal abundance, which

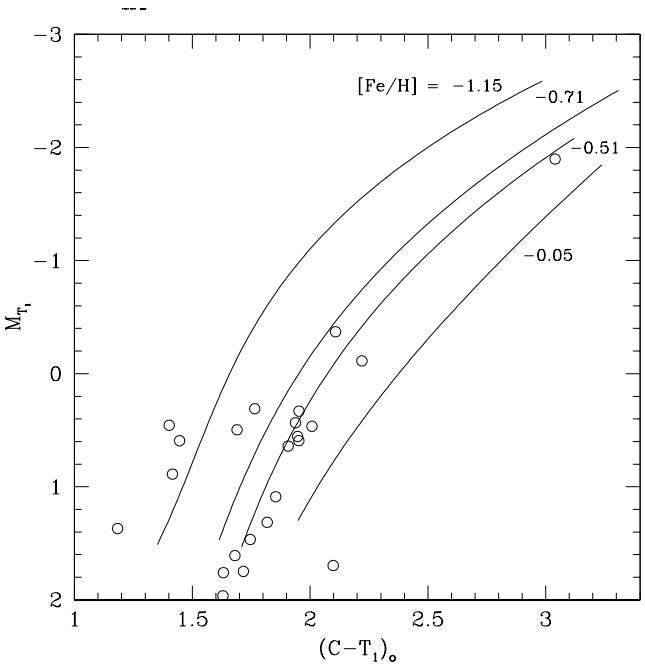

Figure 14. Washington M_{T_1} versus $(C-T_1)_o$ diagram of cluster giant stars in the innermost extracted CMD, with standard giant branches from Geisler & Sarajedini (1999) superimposed. Note that an age-dependent correction to the indicated metallicities, as derived in the text, was applied for Tr 5.

is in full accordance with the results coming from the isochrones matching.

5 DISCUSSION

Tr 5 proved to be a reddened open cluster located near the Galactic plane in the outer disc towards the Galactic anticentre direction.

Our mean $E(B-V)$ colour excess, determined from the innermost cleaned extracted CMDs, is in excellent agreement with the reddening estimates of K98 and KS03. The cluster presents differential interstellar extinction [$\Delta E(B-V) = 0.11$–0.22] caused by an obscure cloud of interstellar matter which covers its southwestern side, the cluster core region ($r < 30$ pixels) being practically unaffected by this cloud. Such differential reddening is not unexpected given its low Galactic latitude ($b = 1\overset{\circ}{.}05$). K98 data also account for differential reddening effect, particularly his *BV* photometry, which was obtained from a larger area than the *VI* one (see Figs. 1 of K98 and KS03). As a matter of fact, the smaller breadth of the K98's cluster MS in the $(V, V-I)$ CMD results from the availability of *VI* data only for the cluster core region. Tilted RGCs are also visible in the K98's $(V, B-V)$ CMD. However, neither of these two studies mention this manifest effect.

The present cluster distance places Tr 5 between 0.5 and 1.0 kpc closer to the Sun than the distances previously derived by K98 and KS03. K98 and KS03 also determined ages and metallicities for the cluster using the same CCD *BVI* data set, but their results significantly differ one from the other. While K98 compares Tr 5 with M67 in age and metallicity, KS03 claim for the cluster a lower age ($t = 2.4 \pm 0.2$ Gyr) and a lower metal content ([Fe/H] $= -0.30 \pm 0.10$). These different results might be reflecting the difficulties in accurately measuring the mean magnitudes of the RGC and the TO on which the above authors based their cluster property determinations. According to the present study, Tr 5 is an old, metal-poor open cluster.

The field stars distributed along the cluster's line of sight appear to be younger on average and somewhat less reddened than the cluster stars. Indeed, the fiducial field star MS (Fig. 7) is ∼10–15 per cent bluer than the cluster MS, which suggests that most of the cluster absorption is also produced in front of the foreground field stars. On the other hand, the less curved MS and the brighter RGC of field stars suggests that the cluster is located behind a younger disc component.

6 CONCLUSIONS

We have presented CCD $VI_{\rm KC}$ photometry of 5094 stars in the field of the old open cluster Tr 5 as well as CCD photometry in the Washington system *C* and T_1 passbands of 2953 stars. The primary results from this study are summarized as follows.

(1) The observed $(V, V-I)$ and $(T_1, C-T_1)$ CMDs, corrected by field star contamination, show a broad MS and a group of red giant clump stars at $(V, V-I) \approx (15.0, 1.8)$ and $(T_1, C-T_1) \approx (14.3, 2.9)$, respectively. We show that the broadness of the cluster MS is mainly a result of the existence of differential reddening across the cluster field.

(2) Estimates of the cluster fundamental parameters were made from comparison of the observed $(V, V-I)$ and $(T_1, C-T_1)$ CMDs with theoretical isochrones of the Geneva group. Cluster age and metallicity were also derived from the δV and δT_1 indices and the standard giant branches of Geisler & Sarajedini (1999), respectively. The following values for the reddening, true distance modulus, age, and metallicity are derived: $E(V-I) = 0.80 \pm 0.05$, $E(C-T_1) = 1.17 \pm 0.15$, $V_{\rm o} - M_V = 11.88 \pm 0.30$ (corresponding to $d = 2.4 \pm 0.5$ kpc), $t = 5.0 \pm 0.5$ Gyr and [Fe/H] $= -0.30 \pm 0.15$. Therefore, Tr 5 turned out to be an old and metal-poor open cluster, located between 0.5 and 1.0 kpc closer to the Sun than previously believed. Star counts carried out within and outside the cluster field reveal that it extends out to an angular radius of 7.7 arcmin, equivalent to a linear radius of 5.4 kpc.

ACKNOWLEDGMENTS

We are gratefully indebted to the CTIO staff for their hospitality and support during the observing run. We also thank the referee for his/her suggestions, which have allowed us to improve the manuscript. This work was partially supported by the Argentinian institutions CONICET, SECYT (Universidad Nacional de Córdoba), Agencia Córdoba Ciencia and Agencia Nacional de Promoción Científica y Tecnológica (ANPCyT). This work is based on observations made at Cerro Tololo Inter-American Observatory, which is operated by AURA, Inc., under cooperative agreement with the NSF.

REFERENCES

Bertelli G., Bressan A., Chiosi C., Fagotto F., Nasi E., 1994, A&AS, 106, 275
Burki G., 1975, A&A, 43, 37
Canterna R., 1976, AJ, 81, 228
Carraro G., Chiosi C., 1994, A&A, 287, 761
Chen L., Hou J. L., Wang J. J., 2003, AJ, 125, 1397
Collinder P., 1931, Medd. Lunds. Astron. Obs. 2
Cousins A. W. J., 1978, Mon. Not. Astron. Soc. S. Afr., 37, 62
Da Costa G. S., Armandroff T. E., 1990, AJ, 100, 162
Dow M. J., Hawarden T. G., 1970, Mon. Not. Astron. Soc. S. Africa, 29, 137
Friel E. D., 1995, ARA&A, 33, 381
Friel E. D., Janes K. A., 1993, A&A, 267, 75
Friel E. D., Janes K. A., Tavarez M., Scott J., Katsanis R., Lotz J., Hong L., Nathan M., 2002, AJ, 124, 2693
Geisler D., 1996, AJ, 111, 480
Geisler D., Bica E., Dottori H., Clariá J. J., Piatti A. E., Santos J. F. C., Jr, 1997, AJ, 114, 1920
Geisler D., Lee M. G., Kim E., 1996, AJ, 111, 1529
Geisler D., Piatti A. E., Bica E., Clariá J. J., 2003, MNRAS, 341, 771
Geisler D., Sarajedini A., 1999, AJ, 117, 308
Janes K. A., Adler D., 1982, ApJS, 49, 425
Janes K. A., Phelps R. L., 1994, AJ, 108, 1773
Kalinowski J. K., 1974, IAU Inf. Bull. Var. Stars 924
Kalinowski J. K., 1975, BAAS, 7, 542
Kalinowski J. K., 1979, PhD thesis, Indiana University
Kalinowski J. K., Burkhead M. S., Honeycutt R. K., 1974, ApJ, 193, L77
Kaluzny J., 1998, A&AS, 133, 25 (K98)
Kim S. C., Sung H., 2003, J. Korean Astron. Soc., 36, 13 (KS03)
King I. R., 1964, Roy. Obs. Bull., 82, 106
Landolt A. U., 1992, AJ, 104, 340
Lejeune T., Schaerer D., 2001, A&A, 366, 538 (LS01)
Phelps R. L., Janes, K. A., Montgomery K. A., 1994, AJ, 107, 1079
Piatti A. E., Clariá J. J., Abadi M. G., 1995, AJ, 110, 2813
Piatti A. E., Clariá J. J., Ahumada A. V., 2003a, MNRAS, 340, 1249 (Paper I)
Piatti A. E., Clariá J. J., Ahumada A. V., 2003b, MNRAS, 346, 390
Piccirillo J., Kalinowski J. K., Wing R. F., 1977, BAAS, 9, 637
Ruprecht J., 1966, Bull. Astron. Inst. Czech., 17, 33
Sandage A. R., 1988, in Philip A. G. D. Davis L., eds, Calibration of Stellar ages. Schenectady, USA, p. 43
Spitzer L., 1988, ApJ, 127, 544
Stetson P. B., 1987, PASP, 99, 191
Strobel A., 1991, A&A, 247, 35
Trumpler R. J., 1930, Lick Obs. Bull., 14, 154

This paper has been typeset from a TEX/LATEX file prepared by the author.